Environmental Science and Pollution Research
https://doi.org/10.1007/s11356-018-2223-8

RESEARCH ARTICLE

# Removal of urea from dilute streams using RVC/nano-$NiO_x$-modified electrode

Reham H. Tammam [1] · Ahmed H. Touny [2,3] · Mahmoud M. Saleh [1,3]

Received: 14 February 2018 / Accepted: 3 May 2018


## Abstract

Reticulated vitreous carbon (RVC), a high surface area electrode (40 $cm^2/cm^3$), has been modified with nickel oxide nanoparticles (nano-$NiO_x$) and used for electrochemical oxidation of urea from alkaline solution. For the cyclic voltammetry measurements, the used dimensions are 0.8 cm × 0.8 cm × 0.3 cm. The purpose was to offer high specific surface area using a porous open network structure to accelerate the electrochemical conversion. $NiO_x$ nanoparticles have been synthesized via an electrochemical route at some experimental conditions. The morphological, structural, and electrochemical properties of the RVC/nano-$NiO_x$ are characterized by using scanning electron microscopy (SEM), energy dispersive X-ray spectroscopy (EDX), cyclic voltammetry (CV), and potentiostatic measurements. The fabricated electrode, RVC/nano-$NiO_x$, demonstrates high electrocatalytic activity towards urea oxidation in an alkaline electrolyte. The onset potential of the RVC/nano-$NiO_x$ compared to that of the planar GC/$NiO_x$ is shifted to more negative value with higher specific activity. The different loadings of the $NiO_x$ have a substantial influence on the conversion of urea which has been evaluated from concentration-time curves. The urea concentration decreases with time to a limit dependent on the loading extent. Maximum conversion is obtained at 0.86 mg of $NiO_x$ per $cm^3$ of the RVC matrix.

**Keywords** RVC · Nickel · Nanoparticles · Urea · Catalysis · Water

## Introduction

Electrochemical oxidation of urea from aqueous solutions has multiple functions. In one side, it can be used as an anodic reaction in what is so-called direct urea fuel cells. In the other side, it can be used for conversion of urea into nontoxic species (Zuo et al. 2015; Mahmoud et al. 2013; Martínez and Bahena 2009; Wang et al. 2017). Also, it can be considered as a base for urea biosensors (Komab et al. 1997). The conversion of urea by electrochemical oxidation can be considered as a fascinating phenomenon for the production of fuel (hydrogen gas) (Simka et al. 2007; Hernández et al. 2014). Interestingly, it is possible to say that the oxidation of urea is not only to remove it from waste streams but also to provide a possible way to produce fuel for fuel cells or any industrials processes that require pure hydrogen gas. For the purpose of the above oxidation process, many electrocatalysts have been used during the last decade.

It has been found that the water electrolysis in an alkaline electrolyte without urea solution differs from that of the one containing urea. Generally, water electrolysis in alkaline electrolytes in the presence of urea demonstrates lower cell voltages compared to that in absence of urea. This unique finding in the presence of urea was attributed the voltage requirements of the process. For hydrogen production via electrolytic cell containing urea (see Eqs. 1–3), the theoretical overall cell potential is 0.082 V. However, it was stated that this value is much less than the corresponding value for water electrolysis in the absence of urea (1.23 V). The above water electrolysis in the presence of urea in alkaline solution can be presented by the following equations (Urbańczyk et al. 2016; Vedharathinam and Botte 2012):

Responsible editor: Bingcai Pan

✉ Mahmoud M. Saleh
mahmoudsaleh90@yahoo.com

[1] Department of Chemistry, Faculty of Science, Cairo University, Cairo, Egypt

[2] Department of Chemistry, Faculty of Science, Helwan University, Helwan, Egypt

[3] Department of Chemistry, College of Science, King Faisal University, Al-Hassa, Kingdom of Saudi Arabia

Published online: 08 May 2018

Anode:

$$CO(NH_2)_{2(aq)} + 6OH^- \rightarrow N_{2(g)} + 5H_2O_{(l)} + CO_{2(g)} + 6e^- \quad E^o = -0.746\ V\ (SHE) \tag{1}$$

Cathode:

$$6H_2O_{(l)} + 6e^- \rightarrow 3H_{2(g)} + 6OH^- \quad E^o = -0.828\ V\ (SHE) \tag{2}$$

Overall:

$$CO(NH_2)_{2(aq)} + H_2O_{(l)} \rightarrow N_{2(g)} + 3H_{2(g)} + CO_{2(g)} \quad E^o = 0.082\ V\ (SHE) \tag{3}$$

Because of the above argument, high electrolytic rates of urea oxidation are considered as an important concern and hence the quest for efficient electrode materials is the main topic of various literatures in the last decade. Although noble metal catalysts such as Pt and Pt-based electrodes have been used for electrochemical oxidation of urea, their possible poisoning and elevated costs were found to decline their applications (Patzer et al. 1991; Xu et al. 2013; Guo et al. 2016). In this context, the research has never ceased to study possible ways of partial or full replacement of the noble catalysts. Among these substituents, metal oxides such as NiO, $Fe_3O_4$, ZnO, and $Cr_2O_3$ represent an important category (Theis 2016; Liu et al. 2018; Lohrasbi and Asgari 2015).

High surface area-to-volume ratio has always been an ultimate factor to increase the rate of an electrochemical reaction (Recio et al. 2011; Guo et al. 2008). However, this topic is considered to be scarce in case of electrochemical oxidation of urea from aqueous alkaline solutions (Ye et al. 2015). Reticulated vitreous carbon (RVC) can offer such property after its modification with nickel nanoparticles. RVC has many distinctive properties such as high surface/volume ratio, high conductivity, low density, high porosity, and stability in acid and alkaline solutions (Saleh et al. 2007; Roh 2008; Maruyama and Abe 2002; Valik et al. 2004). The above features designate such material to be a good candidate in several significant applications. RVC has been known of its applications in many electrochemical systems. These include the removal of organic and inorganic species from dilute streams (Valdez et al. 2012; Windner et al. 1998; Maltosz and Newman 1986; Yan et al. 2012), capacitors (Ramírez et al. 2016; Dalmolin et al. 2010), batteries (Czerwiński et al. 2010), electrolyzers (Walsh et al. 2016; Dell'Era et al. 2014), and sensors (Lepage et al. 2012; Razumas et al. 1994; Yu et al. 2009). Nickel oxide can be the oxide of choice since it is not expensive and abundant. Basically, $NiO_x$ in alkaline solution can easily mediate the electrochemical oxidation of small organic molecules (e.g., urea) at lower potentials via forming $Ni(OH)_2$/NiOOH (i.e., Ni(II)/Ni(III)) couple according to the following equation (Yan et al. 2012):

$$Ni(II) \rightarrow Ni(III) + 1e^- \tag{4}$$

$$Ni(III) + urea \rightarrow Products + Ni(II) \tag{5}$$

Based on the above considerations, there are several goals that will be reported in this study. The main target of the present work is to modify RVC, an electrode of high surface area, with $NiO_x$ nanoparticles. The characterizations of the material, RVC/nano-$NiO_x$ will be done with scanning electron microscopy (SEM) and energy dispersive X-ray spectroscopy (EDX), and the electrochemical oxidation of urea in alkaline solution. The results obtained on RVC/nano-$NiO_x$ will be compared with those obtained on planar GC/nano-$NiO_x$ electrode.

## Experimental

### Reagents and materials

All chemical reagents were of analytical grade, purchased from Merck, and used as received without further purification. Double distilled water was used for preparation of all solutions. The RVC blocks were supplied by ERG Materials and Aero Space Corporation, USA. The RVC blocks were delivered as large blocks and they were cut to the desired dimensions. The RVC was of 60 pore per linear inch (PPI) with a specific area of 40 $cm^2/cm^3$. The ohmic resistance is < 0.01 Ω with porosity of 0.90. The planar glassy carbon electrode (GC) electrode ($d$ = 3 mm) was delivered from BAS Inc., Japan.

### Preparation of RVC/nano-$NiO_x$

The electrodeposition of $NiO_x$ nanoparticles was prepared by a method which was prescribed previously (El-Refaei et al. 2013a, b). It can be processed with two steps: The first one is the electrodeposition of nickel on RVC using a potentiostatic technique in bath containing 5 mM $Ni(NO_3)_2 \cdot 6H_2O$ by applying a constant potential of − 1 V for various time durations in stirred solutions. The second is the passivation of the metallic nickel in 0.1 M phosphate buffer solution (PBS, pH = 7) by using a potential cycling for 10 cycles at the potential range between − 0.3 and 1.1 V with a scan rate of 200 mV/s. Activation of the $NiO_x$ was achieved by potential cycling of the electrode in 1 M NaOH for 20 cycles in the range of − 0.1 to 0.6 V. For comparison, the same procedure was used for the fabrication of GC electrode modified with $NiO_x$ nanoparticles.

### Electrochemical measurements

The used cell in this study consists of an ordinary three-electrode cell comprising the RVC used as the working electrode, platinum coil which was used as a counter electrode, and $Hg/Hg_2Cl_2/KCl$ (sat) (SCE) used as a reference electrode. The cyclic voltammetry response (CV) was measured in the potential range of − 0.1 to 0.6 V (SCE) at different potential scan rates ranging from 5 to 200 mV $s^{-1}$. Stock solution of 1 M urea in 1 M NaOH was prepared and proper dilutions in 1 M NaOH were done to prepare the desired urea solutions. The electrochemical oxidation of urea was carried out in 1 M NaOH containing urea. The reproducibility of the results was confirmed by repeating some experiments at specific conditions. All experiments were done on IM6 ZAHNER-elektrik workstation, Germany, connected to Thales software for *I*/*E* data analyses. The SEM for the samples were carried out using SEM Model Quanta 250 FEG (Field Emission Gun) which was connected to an EDX Unit, with an accelerating voltage of 30 kV, FEI company, Netherlands.

## Results and discussion

### Characterization of the RVC/nano-$NiO_x$

Electrodeposition of $NiO_x$ onto the RVC matrix was achieved according the process details given in the Experimental section. After the electrodeposition of nickel, it was electropassivated by potential cycling in phosphate buffer (pH = 7) in the potential range of − 0.3 to 1.1 V for 10 cycles. Figure 1 shows representative diagram of such successive cycles for RVC/nano-$NiO_x$ with a loading extent of 0.15 mg $cm^{-3}$ (of the RVC volume) at a scan rate of 200 mV $s^{-1}$. The figure reveals an oxidation peak in the first cycle. This corresponds to an active anodic process resulting in dissolution and passivation of the electrodeposited nickel. Simultaneously in the successive cycles, there is a concurrent phase transformation between the different forms of the nickel oxides (El-Refaei et al. 2013a, b). The current decreases during the successive CVs until it reaches low values indicating a formation of passive nickel oxide film. Note that the absence of a cathodic peak means that the formed nickel oxide film is stable within the applied potential range. The above results are similar to that obtained for electrodeposition and passivation of metallic nickel on a planar glassy carbon electrode (Tammam et al. 2015).

The micromorphological structures of the bare RVC and RVC/nano-$NiO_x$ were characterized using field emission scanning electron microscopy. Figure 2 depicts the FE-SEM images for bare RVC (images a and b with different magnifications) and nickel oxide particles electrodeposited on RVC (image c) with a loading extent of 0.15 mg $cm^{-3}$. Image a shows the morphological structure of the bare RVC at low magnification and interlinked thread-like structure of RVC matrix has been displayed. The image also reveals the porous structure of the RVC. An open network structure with 200 μm in length for one network cell and the thickness of one thread equals 50 μm have been revealed. Image b exhibits the morphological structure of the bare RVC at higher magnification and the image does not show any significant surface features. The open structure of the porous matrix provides high access to the electrodeposition of nickel onto the RVC matrix. Image c shows that the $NiO_x$ nanoparticles are distributed on the RVC matrix with a semispherical shape of average particle size of 80 nm. There are uniform distributions of the particles within the RVC matrix. One more image is the EDX chart shown in Fig. 2d. The peaks characteristics of Ni are shown mainly at 0.8 and 7.6 which confirm the nickel structure in the RVC matrix.

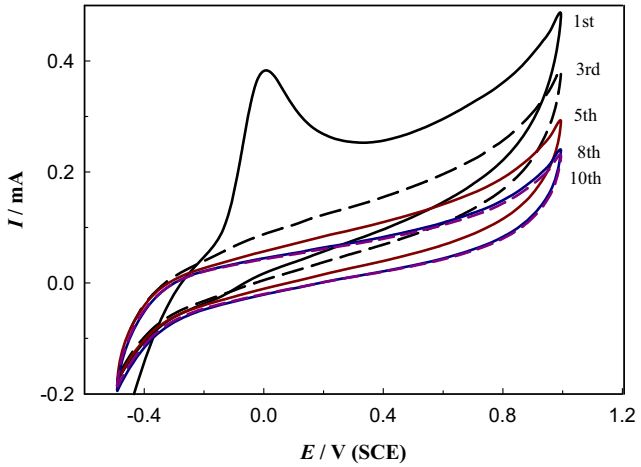


**Fig. 1** Representative diagram of successive cycles of RVC/nano-$NiO_x$ with a loading extent of 0.15 mg $cm^{-3}$ at a scan rate of 200 mV $s^{-1}$ in 0.1 M PBS (pH = 7). Only the first, third, fifth, eighth, and tenth cycles are shown

Activation of the RVC/nano-$NiO_x$ is necessary for emerging of active nickel species (NiOOH and $Ni(OH)_2$) which are required for the electrochemical oxidation of urea. This was done by the activation of the above-formed $NiO_x$ by potential cycling in alkaline solution. Figure 3 depicts the successive CVs of the RVC/nano-$NiO_x$ in 1 M NaOH at the potential range of -0.1 to 0.6 V at the scan rate of 100 mV $s^{-1}$. It was observed that the anodic and cathodic peaks become more obvious with the increase of the potential cycles. The peak current increases before it is stabilized at a cycle number 20 as a couple of peaks. This is attributed to the formation of a redox couple of $Ni(OH)_2$/NiOOH (i.e., Ni(II)/Ni(III)) according to the following equation:

$$Ni(OH)_2 + OH^- \rightleftarrows NiOOH + H_2O + e^- \quad (6)$$

The above-activated electrode was characterized by taking CV responses at different scan rates in the range of 5

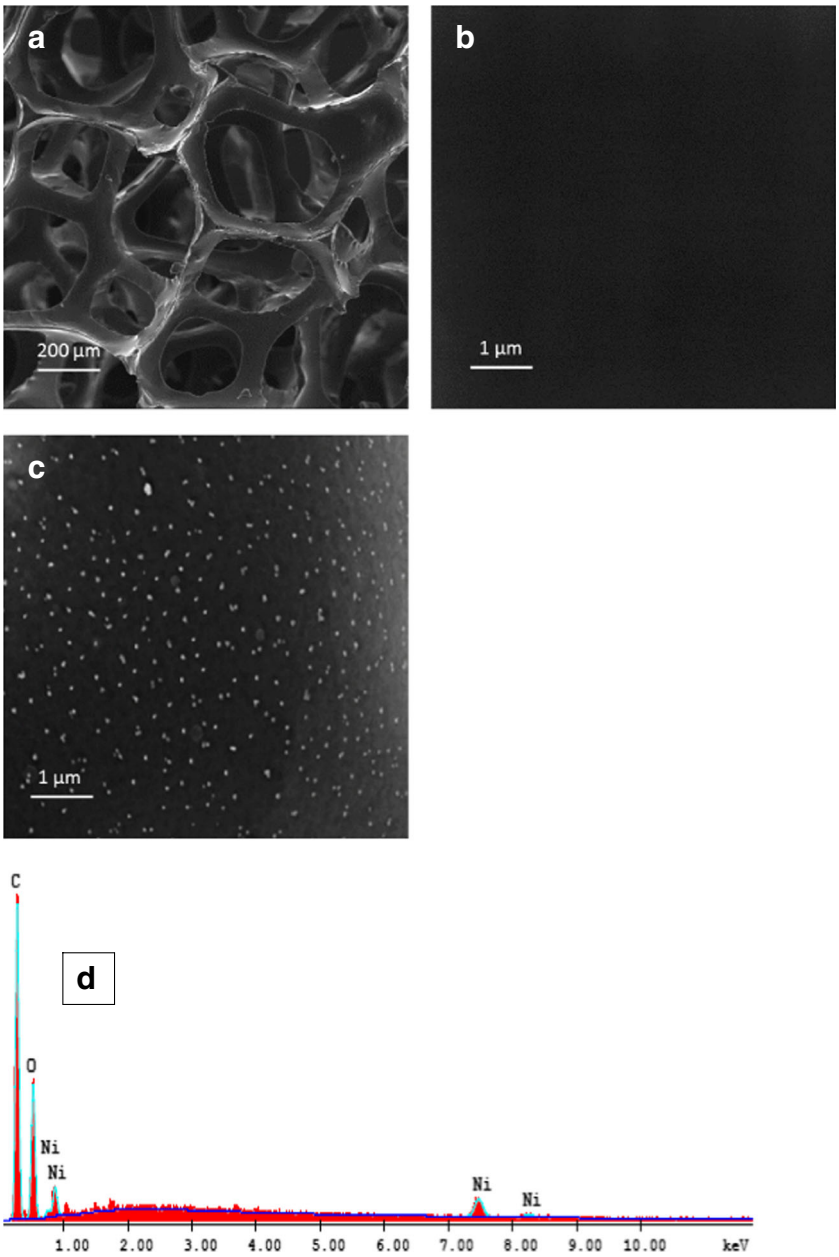


**Fig. 2** SEM images of bare RVC (subpanels **a** and **b** with different magnifications) and nickel oxide particles electrodeposited on RVC (**c**). EDX is shown in panel **d**

to 200 mV $s^{-1}$ for RVC/nano-$NiO_x$ with loading of 0.15 mg $cm^{-3}$. Figure 4a shows such CV responses. As the scan rate increases, the peak current increases both in the anodic and cathodic scans. Note that peaks are not sharp like that obtained at planar electrode (Tammam et al. 2015). The broad peaks are considered as characteristics of porous and high surface area electrodes (Saleh et al. 2007). The anodic peak potential shifts to more positive values and the cathodic peak potential shifts to more negative values. Also, the values of the cathodic peak current are less than that of the anodic peak currents. The above results can be assigned for a quasi-reversible nature of the Ni(II)/Ni(III) transformation. Further discussion of Fig. 4a may be given here to analyze the obtained data. A straight line plot of the peak current, $I_p$, with the square root of the scan rate implies a diffusion-controlled electrochemical reaction and a straight line plot of the $I_p$ with the scan rate implies a surface-confined process (Bockris and Khan 1993). As can be seen in Fig. 4b, a plot of $I_p$ in the anodic and cathodic scans with the scan rate demonstrates straight lines. This may be attributed to a surface-confined process.

## Electrochemical oxidation of urea on RVC/nano-$NiO_x$

The synthesized RVC/nano-$NiO_x$ is applied here for electrochemical oxidation of urea from alkaline solution at different

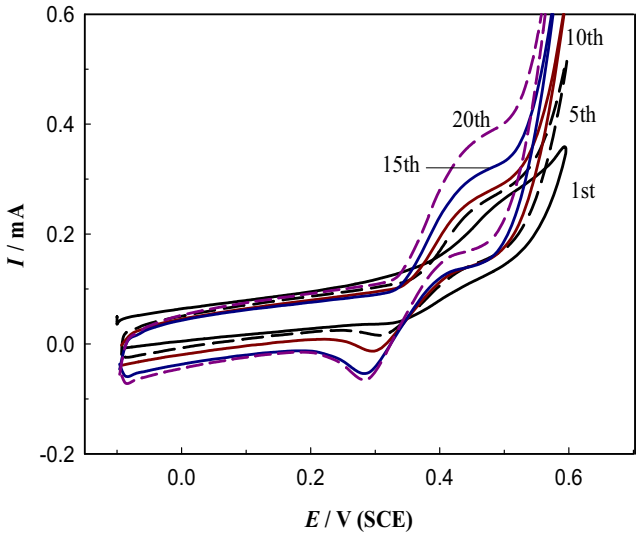


**Fig. 3** Potential cycling of the RVC/nano-$NiO_x$ in 1 M NaOH at the potential range of 0.1 to 0.6 V for 20 cycles

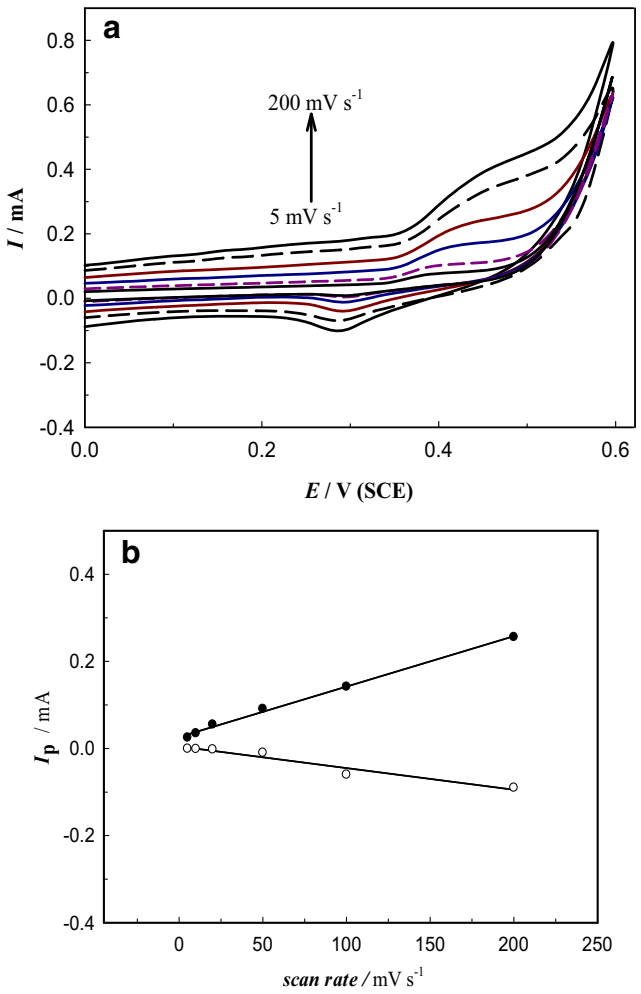


**Fig. 4** **a** CVs of RVC/nano-$NiO_x$ at different scan rates from 5 to 200 mV $s^{-1}$ (from inner to outer = 5, 10, 20, 50, 100, and 200 mV $s^{-1}$) with loading of 0.15 mg $cm^{-3}$ in 1 M NaOH. **b** $I_p$ in the anodic and cathodic sweeps with the scan rate

experimental conditions. Some results of the planar GC/nano-$NiO_x$ electrode will be presented for comparison. Figure 5a represents CVs for bare RVC (curves a and a′) and RVC/nano-$NiO_x$ (0.38 mg $cm^{-3}$) (curves b and b′) in blank 1 M NaOH (curves a and b) and in 1 M NaOH containing 0.3 M urea (curves a′ and b′) at a potential scan rate of 100 mV $s^{-1}$. The CVs demonstrate that bare RVC does not have any considerable activity towards electrochemical oxidation of urea and no apparent features have been shown. Curve b shows two broad peaks (one anodic and one cathodic) which were assigned before for the redox couple (Ni(II)/Ni(III)) given in Eq. 4. In curve b′, in the presence of urea, the CV shows one anodic peak at $E = 0.52$ V with much higher peak current than that obtained in blank. This is assigned for the urea electrooxidation. In the reverse sweep (see arrows) and in the presence of urea, another anodic peak at almost the same potential ($E = 0.5$ V) but with lower peak current is shown. It can be attributed to further urea oxidation. The lower currents indicate non-complete recovery of the Ni active species by the higher anodic potentials. It can be noted that the cathodic peak current corresponding to reduction of Ni(III) to Ni(II) diminishes with respect to that in blank (see curve b). This may be attributed to the consumption of Ni(III) during urea oxidation. The above results may enable us to conclude that urea oxidation on RVC/nano-$NiO_x$ is of an electrocatalytic nature. In Fig. 5b, similar CVs with the same notations and labels are shown for the planar electrode, i.e., GC/nano-$NiO_x$. The results of the planar electrode are presented here for comparison. The $NiO_x$ loading in this figure is 0.45 mg $cm^{-2}$. The general features in the two figures (a and b) are similar. However, there are some differences. The peak of the redox couple, Ni(II)/Ni(III), is broad in the porous electrode but it is normal (sharp) in the case of the planar GC/nano-$NiO_x$ electrode. The capacitance (non-Faradaic) current, i.e., before the peaks, is higher in case of RVC/nano-$NiO_x$ than that occurred in case of the planar GC/nano-$NiO_x$ electrode. One important difference is that the onset potential, $E_{onst}$, of the urea oxidation on the RVC/nano-$NiO_x$ is shifted to a more negative value compared to GC/nano-$NiO_x$. For instance, $E_{onst}$ for urea oxidation is 0.31 and 0.36 at RVC/nano-$NiO_x$ and GC/nano-$NiO_x$, respectively. Also the peak current of urea oxidation on RVC/nano-$NiO_x$ is higher than that on GC/nano-$NiO_x$. For instance, the specific activity of urea oxidation is 19.2 and 11.1 mA $mg^{-1}$ (of the deposited $NiO_x$) at RVC/nano-$NiO_x$ and GC/nano-$NiO_x$, respectively. That is to say, the dispersion of catalyst particles onto a porous matrix can offer better activity towards urea electrocatalytic process.

Figure 6a depicts CV responses of the RVC/nano-$NiO_x$ (loading 0.38 mg $cm^{-3}$) in 1 M NaOH containing 0.3 M urea at different scan rates in the range from 5 to 200 mV $s^{-1}$. As the scan rate increases, the peak current increases. The peak potential of urea oxidation shifts to more positive potential. The cathodic peak current corresponding to the Ni(III) ➔

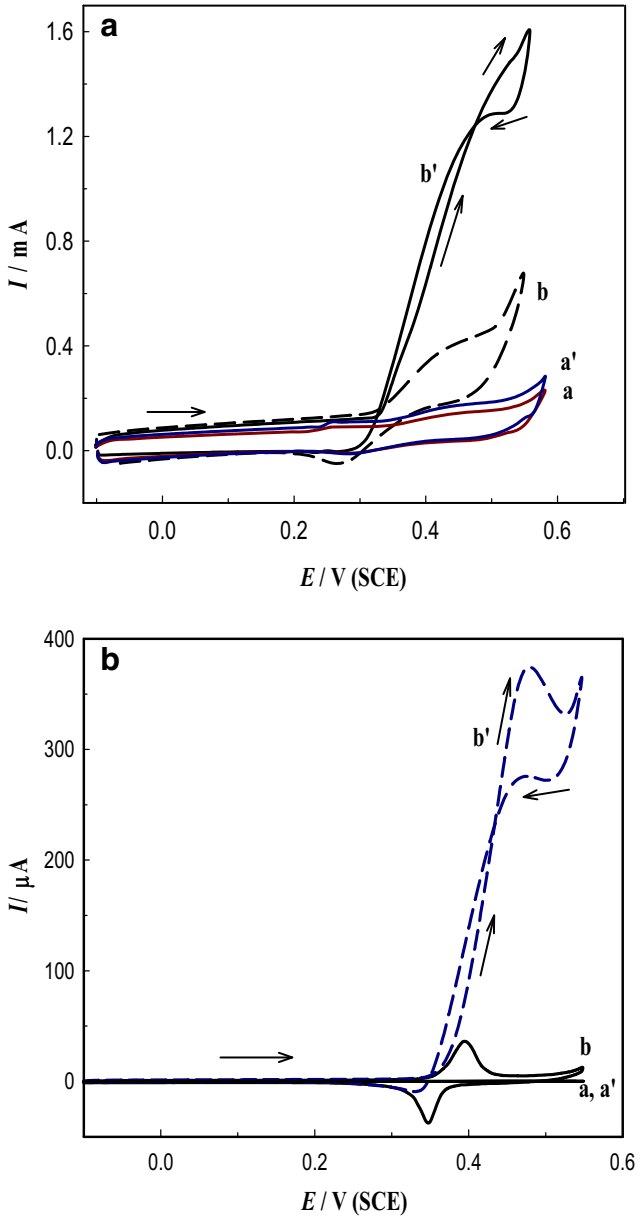


**Fig. 5** **a** CVs of bare RVC (a, a′) and RVC/nano-$NiO_x$ (0.38 mg $cm^{-3}$) (b, b′) in blank 1 M NaOH (a, b) and in 1 M NaOH containing 0.3 M urea (a′, b′) at a potential scan rate of 100 mV $s^{-1}$. **b** The same CV but for bare GC (a, a′) and GC/nano-$NiO_x$ (b, b′) in blank (a, b) and in urea (a′, b′)

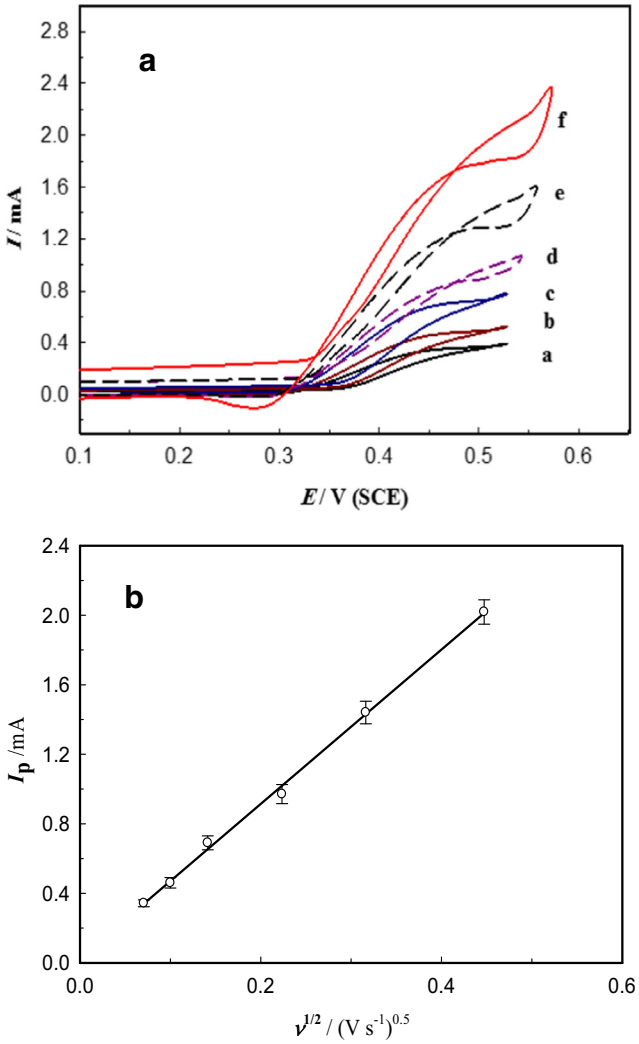


**Fig. 6** **a** CV responses of RVC/nano-$NiO_x$ (0.38 mg $cm^{-3}$) in 1 M NaOH containing 0.3 M urea at different scan rates in the range from 5 to 200 mV $s^{-1}$, (a) 5 mV $s^{-1}$, (b) 10 mV $s^{-1}$, (c) 20 mV $s^{-1}$, (d) 50 mV $s^{-1}$, (e) 100, and (f) 200 mV $s^{-1}$. **b** $I_p$ with the square root of the scan rate

Ni(II) conversion decreases and its decrease depends on the scan rate. That decrease is pronounced at lower scan rate where its relative appearance at higher scan rates points to the slower consumption of Ni(III) with urea. A plot of the peak current with the square rate of the scan rate, $\nu^{0.5}$, is given in Fig. 6b. The plot gives a straight line indicating a diffusion-controlled process. It can be concluded that electrochemical oxidation of urea on the RVC/nano-$NiO_x$ is a totally irreversible diffusion-controlled process. This is in accordance with many literatures at similar conditions but at planar electrodes (El-Khatib and Abdel Hameed 2011; Shi et al. 2017; Vilana et al. 2016).

Optimization of the loading extent of the $NiO_x$ on the RVC matrix is an important issue to be studied. Figure 7 depicts CV responses of urea oxidation on the RVC/nano-$NiO_x$ from 1 M NaOH containing 0.2 M urea at a scan rate of 100 mV $s^{-1}$ and at different loading extents. The extent of loading of the $NiO_x$ was controlled by monitoring the time interval during the electrochemical deposition. Those time intervals applied in the present work were 5, 10, 20, and 40 min. The loading extent in the unit of milligrams per cubic centimeter (of the RVC matrix) was estimated from the amount of charge passed during the electrodeposition process. This was done by subtracting the charge passed in blank (i.e., hydrogen evolution reaction, $Q_{H2}$) from the total charge passed in the presence of 5 mM $Ni^{2+}$ (i.e., [hydrogen evolution reaction + Ni electrodeposition], $Q_{Ni+H2}$). This subtraction gives only the charge of the Ni electrodeposition, $Q_{Ni}$. From the above

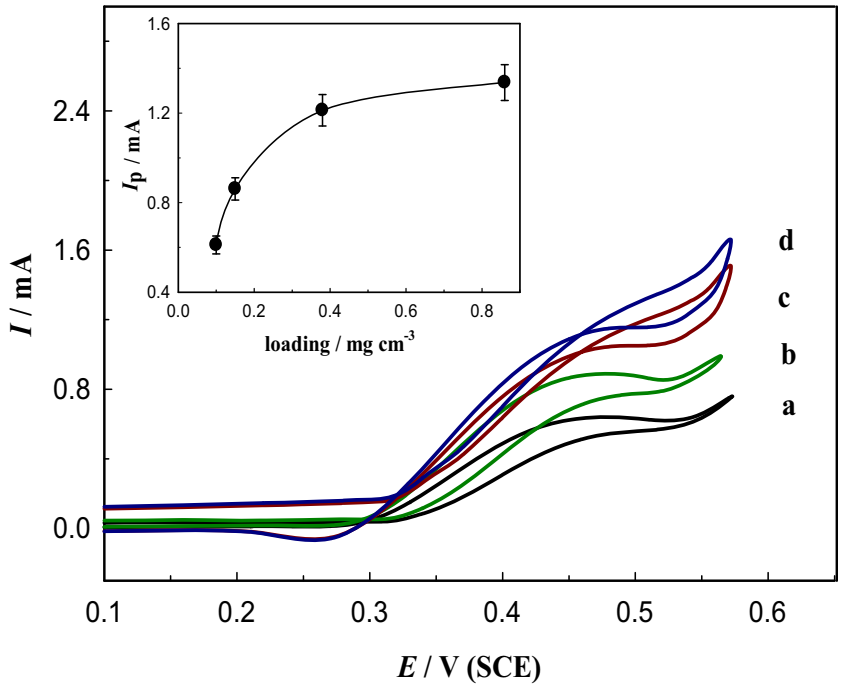


**Fig. 7** CV responses of urea oxidation on RVC/nano-$NiO_x$ from 1 M NaOH containing 0.2 M urea at scan rate of 100 mV $s^{-1}$ at different loading extents. (a) 0.10 mg $cm^{-3}$, (b) 0.15 mg $cm^{-3}$, (c) 0.38 mg $cm^{-3}$, and (d) 0.86 mg $cm^{-3}$. The inset shows $I_p$ with the loading extent

electrodeposition charge and using Faraday's law, the extent of loading was estimated to be 0.10, 0.15, 0.38, and 0.86 mg $cm^{-3}$ (of the RVC volume) for electrodeposition durations of 5, 10, 20, and 40 min, respectively (see Table 1). The CVs shown in Fig. 7 of the urea oxidation imply an increase of the current with the loading extent of the $NiO_x$ up to 20 min (0.38 mg $cm^{-3}$). After this loading, a minor difference in the CVs is noticed. The peak current of urea oxidation, $I_p$, was plotted with the loading extent of the $NiO_x$. This is shown in the inset of Fig. 7. The curve shows that $I_p$ increases with the loading extent until little increase is observed at loading > 0.38 mg $cm^{-3}$. This points to the fact that after loading of 0.38 mg $cm^{-3}$, the electrochemical oxidation of urea is not affected that much by further increase of the $NiO_x$ loading and there is a practical limit for the increase in the loading extent since the reaction is of surface nature. The increase of the peak current is attributed to the increase of the concentration of the nickel species (NiOOH and $Ni(OH)_2$) which result in an increase of the rate of urea oxidation. Since the reaction is a surface reaction and hence depends on the surface concentration of the active Ni species, the extra increase in the bulk loading of $NiO_x$ does not increase the surface reaction by the same amount of increasing the loading extent.

According to our results found here and those obtained from the literatures for urea electrochemical oxidation on planar electrodes modified with nickel species, the mechanism of urea oxidation on RVC/nano-$NiO_x$ can be presented here. Two possible mechanisms can be proposed: the first is the direct oxidation and the second is the indirect or catalyst regeneration (EC′) mechanisms. In the direct oxidation mechanism, urea is oxidized on the surface of the $Ni(OH)_2$-based electrode. The indirect oxidation or catalyst regeneration (EC′) mechanism of urea on RVC/nano-$NiO_x$ catalyst is shown below (Vedharathinam and Botte 2012; Yan et al. 2012).

At the anode:

$$\mathrm{E}\ 6\mathrm{Ni(OH)_{2(s)}} + 6\mathrm{OH^-} \leftrightharpoons 6\mathrm{NiOOH_{(s)}} + 6\mathrm{H_2O_{(l)}} + 6\mathrm{e^-} \quad (7)$$

$$\mathrm{C}\ 6\mathrm{NiOOH_{(s)}} + \mathrm{CO(NH_2)_{2(aq)}} + \mathrm{H_2O_{(l)}} \rightarrow 6\mathrm{Ni(OH)_{2(s)}} + \mathrm{N_{2(g)}} + \mathrm{CO_{2(g)}} \quad (8)$$

Net anodic reaction:

$$\mathrm{EC'}\ \mathrm{CO(NH_2)_{2(aq)}} + 6\mathrm{OH^-} \rightarrow \mathrm{N_{2(g)}} + 5\mathrm{H_2O_{(l)}} + \mathrm{CO_{2(g)}} + 6\mathrm{e^-} \quad (9)$$

**Table 1** Total charge consumed during nickel deposition, $Q_{Ni+H2}$ ($Ni^{2+}$-containing bath), during hydrogen evolution reaction, $Q_{H2}$ ($Ni^{2+}$-free bath), and loading extent at RVC electrode at different time durations

| *t*/min | $Q_{H2}$/mC | $Q_{Ni+H2}$/mC | $Q_{Ni}$/mC | Loading/mg $cm^{-3}$ |
|---|---|---|---|---|
| 5 | 10.5 | 72.9 | 62.5 | 0.10 |
| 10 | 19.1 | 112.5 | 93.4 | 0.15 |
| 20 | 35.2 | 275.6 | 240.3 | 0.38 |
| 40 | 64.5 | 603.7 | 539.2 | 0.86 |

The above mechanism implies that $Ni(OH)_2$ is oxidized to catalytically active NiOOH ($Ni^{3+}$) which is chemically reduced to the inactive $Ni(OH)_2$ ($Ni^{2+}$) due to urea oxidation. Consequently, urea is chemically converted to products. At the prevailing anodic potential, the $Ni(OH)_2$ species are converted to the more electrochemically active form NiOOH. Therefore, regeneration of the catalyst for further oxidation of urea can be occurred. This is in accordance with the results shown in Fig. 5. One can conclude that the transformation of the redox couple NiOOH/$Ni(OH)_2$ is a reversible process (see Fig. 3) in the present alkaline solution. However, as it was concluded from Fig. 5 the presence of urea in the alkaline electrolyte converts NiOOH to $Ni(OH)_2$ and is regenerated according to:

$$Ni(OH)_{2(s)} + OH^- \rightleftarrows NiOOH_{(s)} + H_2O_{(l)} + e^- \quad (10)$$

$$NiOOH_{(s)} + urea_{(aq)} \rightarrow Ni(OH)_{2(s)} + products \quad (11)$$

The above two equations imply the catalyst regeneration as per the indirect oxidation of urea (Vedharathinam and Botte 2012; Yan et al. 2012).

It is expected for the high surface area electrode to enhance the rate of the electrochemical reaction. In this context, the present electrode, RVC/nano-$NiO_x$, was applied for conversion of urea from aqueous alkaline solution for some time intervals in order to test its ability to remove a targeted amount of urea. Figure 8 shows concentration-time curves for urea oxidation on RVC/nano-$NiO_x$ at $E = 0.5$ V from stirred 1 M NaOH containing 0.2 M urea of total volume 100 ml. The used loading extents are (a) 0.10, (b) 0.15, (c) 0.38, and (d) 0.86 mg $cm^{-3}$ (of the RVC volume) corresponding to electrodeposition duration of 5, 10, 20, and 40 min, respectively. The dimensions of the RVC electrode are 0.8 cm × 0.8 cm × 0.3 cm. The concentration of urea during the electrolysis was monitored using a planar GC/nano-$NiO_x$ electrode as a probe electrode to measure the concentration of urea with time. The urea concentration was measured with time as follows. A calibration curve was obtained as can be seen in the inset of Fig. 8. This calibration curve was collected on GC/nano-$NiO_x$ in 1 M NaOH containing different urea concentrations by measuring linear sweep voltammogram (LSV) at different concentrations of urea (similar to the CVs in Fig. 5b) in the range of 0.05 to 0.2 M at a scan rate of 10 mV $s^{-1}$. The GC/nano-$NiO_x$ was immersed in the electrolytic cell and LSV was measured at the desired time and the peak current values at different time intervals were used to determine the [urea] at different electrolytic times. The calibration curve enables us to monitor the concentration of urea with time during electrolysis using RVC/nano-$NiO_x$ electrode. Figure 8 demonstrates that after some short induction period (after 5 min), the [Urea] decreases with time with a regime dependent on the loading of the $NiO_x$ on the RVC. Faster decrease is obtained and lower

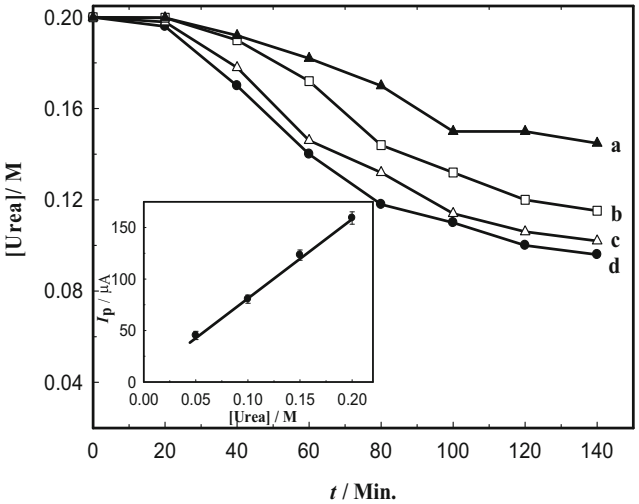


**Fig. 8** Concentration-time curves for urea oxidation on RVC/nano-$NiO_x$ from stirred 1 M NaOH containing 0.2 M urea. The loading extents are (a) 0.10 mg $cm^{-3}$, (b) 0.15 mg $cm^{-3}$, (c) 0.38 mg $cm^{-3}$, and (d) 0.86 mg $cm^{-3}$ (of the RVC volume) and the dimension of the electrode is 0.8 cm × 0.8 cm × 0.3 cm. The inset shows the calibration curve

concentrations of urea are obtained after the first 30 min. It may be concluded that more than 60% of urea was removed after 120 min using the higher loading of $NiO_x$ (0.86 mg $cm^{-3}$). Lower conversions were obtained using lower loadings of $NiO_x$. Generally, the conversion extent of urea increases with the loading extent. However, the increase in the conversion from loading of 0.38 to 0.86 mg $cm^{-3}$ is not significant. This may be due to the surface nature of the electrochemical oxidation of urea. Figure 8 shows that the urea is not completely removed but its concentration reaches to certain lower values that are dependent on the loading extent. This trend may be attributed to the start of poisoning of the electrode with the oxidation products of urea and hence it should be either regenerated or replaced by a fresh electrode in order to obtain complete removal of urea.

## Conclusions

A high surface area substrate (RVC) electrode modified with $NiO_x$ nanoparticles was synthesized and used for electrochemical oxidation of urea from alkaline solution. The RVC/nano-$NiO_x$ was activated by potential cycling in 1 M NaOH in the potential range of 0.1–0.6 V to obtain proper active material. The electrode demonstrates high electrocatalytic activity towards urea oxidation at a peak potential of 0.52 V (SCE). It was characterized by surface and electrochemical tools. The RVC/nano-$NiO_x$ demonstrates high electrocatalytic activity than planar GC/nano-$NiO_x$. This was attributed to the high surface area and open matrix network with higher diffusion and high rates of charge transfer between electroactive species and the analyte (urea). Concentration-time curves were

recorded in order to assess the ability of the electrode to remove urea from dilute solutions at different loadings of the $NiO_x$. Considerable conversion of urea was obtained at higher loadings of $NiO_x$. More than 60% of urea was removed after 120 min using the higher loadings of $NiO_x$ (0.86 mg $cm^{-3}$).

## References


Bockris JOM, Khan SUM (1993) Surface electrochemistry: a molecular level approach. Plenum, New York, p 223

Czerwiński A, Obrębowski S, Kotowski J, Rogulski Z, Skowroński JM, Krawczyk P, Rozmanowski T, Bajsert M, Przystałowski M, Buczkowska-Biniecka M, Jankowsk E, Baraniak M (2010) Electrochemical behavior of negative electrode of lead-acid cells based on reticulated vitreous carbon carrier. J Power Sources 195: 7524–7529

Dalmolin C, Biaggio SR, Rocha-Filho RC, Bocchi N (2010) Reticulated vitreous carbon/polypyrrole composites as electrodes for lithium batteries: preparation, electrochemical characterization and charge–discharge performance. Synth Met 160:173–179

Dell'Era A, Pasquali M, Lupi C, Zaza F (2014) Purification of nickel or cobalt ion containing effluents by electrolysis on reticulated vitreous carbon cathode. Hydrometallurgy 150:1–8

El-Khatib KM, Abdel Hameed RM (2011) Development of $Cu_2O$/Carbon Vulcan XC-72 as non-enzymatic sensor for glucose determination. Biosens Bioelectron 26:3542–3548

El-Refaei SM, Awad MI, El-Anadouli BE, Saleh MM (2013a) Electrocatalytic glucose oxidation at binary catalyst of nickel and manganese oxides nanoparticles modified glassy carbon electrode: optimization of the loading level and order of deposition. Electrochim Acta 92:460–467

El-Refaei SM, Saleh MM, Awad MI (2013b) Enhanced glucose electrooxidation at a binary catalyst of manganese and nickel oxides modified glassy carbon electrode. J Power Sources 223:125–128

Guo Y, Hu J, Wan L (2008) Nanostructured materials for electrochemical energy conversion and storage devices. Adv Mater 20:2878–2887

Guo F, Ye K, Du M, Huang X, Cheng K, Wang G, Cao D (2016) Electrochemical impedance analysis of urea electro-oxidation mechanism on nickel catalyst in alkaline medium. Electrochim Acta 210: 474–482

Hernández MC, Russo N, Panizza M, Spinelli P, Fino D (2014) Electrochemical oxidation of urea in aqueous solutions using a boron-doped thin-film diamond electrode diamond. Relat Mater 44:109–116

Komab S, Seyam M, Momm T, Osaka T (1997) Potentiometric biosensor for urea based on electropolymerized electroinactive polypyrrole. Electrochim Acta 42:383–388

Lepage G, Albernaz FO, Perrier G, Merlin G (2012) Characterization of a microbial fuel cell with reticulated carbon foam electrodes. Bioresour Technol 124:199–207

Liu R, Liu R, Ma X, Davis BH, Li Z (2018) Efficient diesel production over the iron-based Fischer–Tropsch catalyst supported on CNTs treated by urea/NaOH. Fuel 211:827–836

Lohrasbi E, Asgari M (2015) Electrooxidation of urea on the nickel oxide nanoparticles and multi-walled carbon nanotubes modified screen printed electrode. Adv Anal Chem 5:9–18

Mahmoud MH, Abdel-Salam OE, Abdel-Monem NM, Nassar AF, El-Halwany MA (2013) Removal of urea from industrial waste water using electrochemical decomposition. Life Sci J 10:2048–2055

Maltosz M, Newman J (1986) Experimental investigation of a porous carbon electrode for the removal of mercury from contaminated brine. J Elecrochem Soc 133:1850–1859

Martínez SS, Bahena CL (2009) Chlorbromuron urea herbicide removal by electro-Fenton reaction in aqueous effluents. Water Res 43:33–40

Maruyama J, Abe I (2002) Cathodic oxygen reduction at the interface between Nafion® and electrochemically oxidized glassy carbon surfaces. J Electroanal Chem 527:65–70

Patzer JF, Wolfson SKJ, Yao SJ (1991) Platinized-titanium electrodes for urea oxidation Part II. Concentric spiral coil geometry. J Mol Catal 70:231–242

Ramírez G, Javier RF, Herrasti P, Ponce-de-León C, Sirés I (2016) Effect of RVC porosity on the performance of $PbO_2$ composite coatings with titanate nanotubes for the electrochemical oxidation of azo dyes. Electrochim Acta 204:9–17

Razumas V, Kanapienienė J, Nylander T, Engström S, Larsson K (1994) Electrochemical biosensors for glucose, lactate, urea, and creatinine based on enzymes entrapped in a cubic liquid crystalline phase. Anal Chim Acta 289:155–162

Recio FJ, Herrasti P, Sirés L, Kulak AN, Bavykin DV, Ponce-de-León C, Walsh FC (2011) The preparation of $PbO_2$ coatings on reticulated vitreous carbon for the electro-oxidation of organic pollutants. Electrochim Acta 56:5158–5165

Roh H (2008) Characterization of the acoustic properties of random porous media: reticulated vitreous carbon and aluminum foam. J Korean Phys Soc 53:607–616

Saleh MM, Awad MI, Okajima T, Suga K, Ohsaka T (2007) Characterization of oxidized reticulated vitreous carbon electrode for oxygen reduction reaction in acid solutions. Electrochim Acta 52:3095–3104

Shi W, Ding R, Li X, Xu Q, Liu E (2017) Enhanced performance and electrocatalytic kinetics of Ni-Mo/graphene nanocatalysts towards alkaline urea oxidation reaction. Electrochim Acta 242:247–259

Simka W, Piotrowski J, Nawrat G (2007) Influence of anode material on electrochemical decomposition of urea. Electrochim Acta 52:5696–5703

Tammam RH, Fekry AM, Saleh MM (2015) Electrocatalytic oxidation of methanol on ordered binary catalyst of manganese and nickel oxide nanoparticles. Int J Hydrog Energy 40:275–283

Theis JR (2016) An assessment of Pt and Pd model catalysts for low temperature $NO_x$ adsorption. Catal Today 267:93–109

Urbańczyk E, Sowa M, Simka W (2016) Urea removal from aqueous solutions—a review. J Appl Electrochem 46:1011–1029

Valdez HCA, Jiménez GG, Granados SG, Ponce de Leon C (2012) Degradation of paracetamol by advanced oxidation processes using modified reticulated vitreous carbon electrodes with $TiO_2$ and CuO/$TiO_2$/$Al_2O_3$. Chemosphere 89:1195–1201

Valik K, Schiffrin DJ, Tammeveski K (2004) Electrochemical reduction of oxygen on anodically pre-treated and chemically grafted glassy carbon electrodes in alkaline solutions. Elecrochem Commun 6:1–5

Vedharathinam V, Botte GG (2012) Understanding the electro-catalytic oxidation mechanism of urea on nickel electrodes in alkaline medium. Electrochim Acta 81:292–300

Vilana J, Gómez E, Vallés E (2016) Influence of the composition and crystalline phase of electrodeposited CoNi films in the preparation of CoNi oxidized surfaces as electrodes for urea electro-oxidation. Appl Surf Sci 360:816–825

Walsh FC, Arenas LF, Ponce de León C, Reade GW, Whyte I, Mellor BG (2016) The continued development of reticulated vitreous carbon as a versatile electrode material: structure, properties and applications. Electrochim Acta 215:566–591

Wang L, Xie B, Gao N, Min B, Liu H (2017) Urea removal coupled with enhanced electricity generation. Environ Sci Pollut Res 24:20401–20408

Windner RC, Sousa MFB, Bertazzoli R (1998) Electrolytic removal of lead using a flow-through cell with a reticulated vitreous carbon cathode. J Appl Electrochem 28:201–207

Xu X, Zhou Y, Yuan T, Li Y (2013) Methanol electrocatalytic oxidation on Pt nanoparticles on nitrogen doped graphene prepared by the hydrothermal reaction of grapheme oxide with urea. Electrochim Acta 112:587–595

Yan W, Wang D, Botte GG (2012) Electrochemical decomposition of urea with Ni-based catalysts. Appl Catal, B 127:221–226

Ye K, Zhang D, Guo F, Cheng K, Wang G, Cao D (2015) Highly porous nickel carbon sponge as a novel type of three-dimensional anode with low cost for high catalytic performance of urea electro-oxidation in alkaline medium. J Power Sources 283:408–415

Yu J, Tang ZA, Yan GZ, Chan PCH, Huang ZX (2009) An experimental study on micro-gas sensors with strip shape tin oxide thin films. Sensors Actuators B Chem 139:346–352

Zuo L, Zhang Y, Zhang L, Miao Y, Wei F, Liu T (2015) Polymer/carbon-based hybrid aerogels: preparation. Prop Appl Mat 8:6806–6848